European Journal of Immunology
Clinical·Basic·Translational

Immunity to infection

Clinical

Research Article

Distinct and dynamic activation profiles of circulating dendritic cells and monocytes in mild COVID-19 and after yellow fever vaccination

Elena Winheim[#1], *Tabea Eser*[#2,3], *Flora Deák*[2,3], *Mohamed I. M. Ahmed*[2,3], *Olga Baranov*[2,3], *Linus Rinke*[1], *Katharina Eisenächer*[1], *Antonio Santos-Peral*[4,5], *Hadi Karimzadeh*[4,5], *Michael Pritsch*[2,4,5], *Clemens Scherer*[6,8], *Maximilian Muenchhoff*[6,7,3], *Johannes C. Hellmuth*[6,9], *Michael von Bergwelt-Baildon*[6,9], *Laura Olbrich*[2,3], *Michael Hoelscher*[2,3], *Andreas Wieser*[2,3,10], *Inge Kroidl*[2,3], *Simon Rothenfusser*[4,5], *Christof Geldmacher*[2,3] *and Anne B. Krug*[1]

[1] Institute for Immunology, Biomedical Center (BMC), Faculty of Medicine, LMU Munich, Munich, Germany
[2] Division of Infectious Diseases and Tropical Medicine, University HospitalLMU Munich, Munich, Germany
[3] German Center for Infection Research (DZIF), Partner Site Munich, Munich, Germany
[4] Division of Clinical Pharmacology, University HospitalLMU Munich, Munich, Germany
[5] Unit Clinical Pharmacology (EKLiP), Helmholtz Zentrum München, German Research Center for Environmental Health (HMGU), Neuherberg, Germany
[6] COVID-19 Registry of the LMU Munich (CORKUM), University HospitalLMU Munich, Munich, Germany
[7] Max von Pettenkofer Institute of Hygiene and Medical Microbiology, Faculty of Medicine & Gene Center, Virology, National Reference Center for RetrovirusesLMU Munich, Munich, Germany
[8] Department of Medicine I, University HospitalLMU Munich, Munich, Germany
[9] Department of Medicine III, University HospitalLMU Munich, Munich, Germany
[10] Max von Pettenkofer Institute of Hygiene and Medical Microbiology, Faculty of MedicineLMU Munich, Munich, Germany

Dysregulation of the myeloid cell compartment is a feature of severe disease in hospitalized COVID-19 patients. Here, we investigated the response of circulating dendritic cell (DC) and monocyte subpopulations in SARS-CoV-2 infected outpatients with mild disease and compared it to the response of healthy individuals to yellow fever vaccine virus YF17D as a model of a well-coordinated response to viral infection. In SARS-CoV-2-infected outpatients circulating DCs were persistently reduced for several weeks whereas after YF17D vaccination DC numbers were decreased temporarily and rapidly replenished

Correspondence: Anne B. Krug
e-mail: anne.krug@med.uni-muenchen.de

[#]Contributed equally

by increased proliferation until 14 days after vaccination. The majority of COVID-19 outpatients showed high expression of CD86 and PD-L1 in monocytes and DCs early on, resembling the dynamic after YF17D vaccination. In a subgroup of patients, low CD86 and high PD-L1 expression were detected in monocytes and DCs coinciding with symptoms, higher age, and lower lymphocyte counts. This phenotype was similar to that observed in severely ill COVID-19 patients, but less pronounced. Thus, prolonged reduction and dysregulated activation of blood DCs and monocytes were seen in a subgroup of symptomatic non-hospitalized COVID-19 patients while a transient coordinated activation was characteristic for the majority of patients with mild COVID-19 and the response to YF17D vaccination.

Keywords: dendritic cells · monocytes · SARS-CoV-2 · yellow fever · YF17D

Additional supporting information may be found online in the Supporting Information section at the end of the article.

Introduction

Infections with SARS-CoV-2 emerged in 2019 and, due to its highly contagious nature, led to a global pandemic. The clinical presentation of SARS-CoV-2 infections is highly variable, ranging from asymptomatic infections to mild, moderate, and even severe diseases with fatal outcomes. Host factors, such as age, sex, comorbidities, and the quality and dynamic of the immune response have a significant influence on disease progression after infection [1]. In patients who progress to severe disease, the immune response appears to be dysregulated, leading to inflammatory responses and subsequent tissue damage in the lung and other organs. In mild disease cases, the infection is well controlled by the immune system and is either asymptomatic or associated with mild symptoms such as fever or cold-like symptoms without known organ damage. The innate immune response triggered by viral sensors is highly relevant for limiting virus replication and dissemination as well as inducing adaptive immune responses. However, it also causes inflammatory responses that contribute to organ damage. Therefore, the innate immune response is a deciding factor for the course of COVID-19 [2, 3] and other viral infections such as influenza pneumonia [4, 5]. Early innate responses also impact the response to live-virus vaccines [6, 7].

Yellow fever (YF) vaccination using the live-attenuated vaccine virus (YF17D) can be used as a model for controlled viral infections in humans [8]. Alterations in the composition and activation state of circulating myeloid cells and a robust systemic innate immune response dominated by IFN-stimulated genes have been observed in response to YF17D. Interestingly, it was shown that gene expression changes in peripheral blood mononuclear cells (PBMC) indicating strong innate immune responses correlate with and predict adaptive immune responses to vaccination [7, 9]. This highlights the importance of a well-coordinated response of innate immune cells such as dendritic cells (DCs) and monocytes for adaptive immunity.

DCs are professional antigen-presenting cells (APCs) and are highly competent in secreting pro-inflammatory cytokines as well as inducing adaptive immune responses. They are divided into conventional DCs (cDCs) and plasmacytoid DCs (pDCs). While cDC1 are efficient in crosspresenting antigens to $CD8^+$ T cells and promoting their differentiation into cytotoxic T cells, cDC2 are potent inducers of T helper (Th)2 and Th17 responses. Due to their ability to produce large amounts of type I IFNs upon viral stimulation, pDCs are important for innate antiviral immunity and also support antiviral T cell responses. In the peripheral blood of patients with severe COVID-19, the frequency and absolute numbers of pDC and cDC subsets are persistently reduced [10–15]. Phenotypic changes observed in circulating DCs and monocytes of hospitalized COVID-19 patients include reduced expression of HLA-DR and costimulatory molecule CD86 as well as high expression of regulatory molecule programmed death-ligand-1 (PD-L1), a ligand of inhibitory receptor PD-1 expressed on activated T cells. Additionally, DC function was found to be impaired resulting in a reduced capacity to stimulate T cells and a diminished ability to secrete antiviral cytokines [10, 14, 15]. Several studies have described impairment and dysregulation of the innate immune response in hospitalized COVID-19 patients with more severe disease [13, 15, 16], but these results may be confounded by comorbidities and therapeutic interventions and lack information on milder disease courses. Furthermore, studies comparing the innate immune response to SARS-CoV-2 to models of well-controlled viral infections such as YF17D vaccination are lacking. This could elucidate differences in the dynamic and magnitude of the responses and help to identify specific features of immune dysregulation in COVID-19 patients.

Therefore, this study provides a longitudinal analysis of circulating DC and monocyte subset responses in outpatients lacking major comorbidities or therapeutic interventions associated with severe COVID-19 disease manifestations. The response to SARS-CoV-2 is then compared to the well-coordinated response seen in these cell types after yellow fever vaccination that leads to long-lasting protection from infection. Through this comparison, we identified a persistent reduction in circulating DC numbers and a heterogenous activation profile of DCs and monocytes. In

a subset of COVID-19 patients, we identified low CD86 and high PD-L1 expression in DCs and monocytes as characteristic features associated with more symptomatic disease and higher age.

Results

Study design

To analyze the innate immune response to SARS-CoV-2, multiparametric flow cytometric analysis of DC and monocyte subsets was performed using PBMCs freshly isolated from blood of SARS-CoV-2 infected outpatients at several timepoints after primary symptom onset. The patients and their household contacts were longitudinally monitored with nasal swabs and SARS-CoV-2 diagnostic PCR for several months. All patients in this study presented with mild COVID-19 symptoms (score 1–3) without the need for hospitalization (mild, $n = 39$). Participants with SARS-CoV-2 infection were enrolled within 14 days of symptom onset into the KoCo19-Immu study from May to December 2020 in Munich, Germany, before the emergence of variants of concern, and followed during 3 weekly visits until week 4 and two additional visits after 2 months (Fig. 1A, first timepoint 1–7 days after symptom onset, median 5 days). The healthy (H) control group was recruited from household contacts of COVID-19 patients as well as other age-matched donors (healthy = H, $n = 15$, Fig. 1A). Seven hospitalized COVID-19 patients with severe disease (score: 4–8, median score: 8) enrolled in December 2020 were included in this study as a separate group (severe = S, $n = 7$, median 10 days after diagnosis). To compare the innate immune response to SARS-CoV-2 with the response of healthy individuals to YF17D vaccine virus, blood samples were collected from healthy volunteers shortly before and on days 3, 7, and 14 after vaccination and freshly isolated PBMC were analyzed by flow cytometry (orange, $n = 9$–20, Fig. 1A).

Increase of Lineage$^-$ HLA-DR$^+$ cells lacking DC and monocyte markers in PBMC of COVID-19 patients

Previous publications reported a reduction of monocyte and DC frequency in patients with severe COVID-19 manifestations [13]. To analyze this in our cohort, we determined the frequency of monocytes and DCs within the HLA-DR$^+$ Lin$^-$ PBMC fraction at different time points after symptom onset (1-7 [median: 5], 8–14 [11], 15–21 [17], 22–27 [25], 28–35 [32], 36–59 [41.5] and over 60 [68] days) and compared it to that of the healthy control group. As expected, a relative reduction of the percentages of monocytes and DCs of total HLA-DR$^+$ Lin $^-$ cells was observed in COVID-19 patients with severe disease compared to the healthy control group. However, this was not observed in the COVID-19 outpatient group (Fig. 1B, C, gating in supplementary Fig. S1). Concomitantly, nonDCs, which lack typical monocyte and DC markers as well as T, B, NK cell, and granulocyte markers (CD3$^-$, CD14$^-$, CD16$^-$, CD19$^-$, CD20$^-$, CD56$^-$, CD66b$^-$, CD123$^-$, CD11c$^-$, CD1c$^-$, CD141$^-$) but expressing CD86$^{+/-}$ and HLA-DR$^+$, were found to be highly represented in patients suffering from severe disease (Fig. 1B and C; Fig. S2). In outpatients with mild disease, a significant increase of nonDCs was also observed at early time points up to 14 days after symptom onset but was less pronounced than in the hospitalized patients with severe COVID-19 (Fig. 1B and C). In summary, a statistically significant increase of nonDCs was found during both severe disease and early mild COVID-19 while DC and monocyte frequencies were significantly reduced only in patients with severe COVID-19.

Dynamic changes in monocyte and DC subpopulations in COVID-19 patients

Focusing on monocytes, we found an increased percentage of CD14$^+$ CD16$^+$ intermediate monocytes up to 7 days after symptom onset and a reduction of CD14$^-$ CD16$^+$ non-classical monocytes in outpatients with mild disease and in hospitalized patients with severe disease. In patients with severe disease the percentage of CD14$^+$ CD16$^-$ classical monocytes was significantly reduced due to the shift towards intermediate monocytes (Fig. 1D, gating strategy supplementary Fig. S1). No major changes in the composition of the DC compartment were observed (supplementary Fig. S2). To assess the time course of pDC and cDC1 frequencies within individual patients we restricted the analysis to 20 patients of which at least 3 consecutive samples were available. These measurements were grouped into three time points after the onset of symptoms: 0 to 15 days (to 15), 16 to 30 days (to 30), and 31 to 70 days (>30). This analysis revealed great interindividual variability in the dynamic changes of pDC and cDC1 frequencies with a subgroup of patients showing reduced cDC1 frequencies up to 30 days after symptom onset with recovery thereafter (Supplementary Fig. S3). Absolute counts of cDC1, cDC2, and pDCs were significantly reduced at early time points after symptom onset compared to the latest time point while monocyte counts were not significantly altered in the cohort of outpatients with mild COVID-19 (Fig. 1E).

We conclude from these results that outpatients with mild COVID-19 show similar shifts in monocyte subpopulations as observed previously in more severe disease that were most pronounced within the first week after symptom onset. Additionally, a reduction in absolute numbers of pDC and cDC subsets was identified, while DC subset composition was not greatly altered and highly variable between individuals.

Distinct activation and proliferation profile of DCs in mild compared to severe COVID-19 patients

Recruitment of immature immune cells into the circulation was observed after infection with SARS-CoV-2 [13]. Since an expansion of HLA-DR$^+$ cells lacking markers of differentiated DCs and monocytes (nonDCs) was observed, the proliferation of these cells in comparison to DCs and monocytes was measured by staining

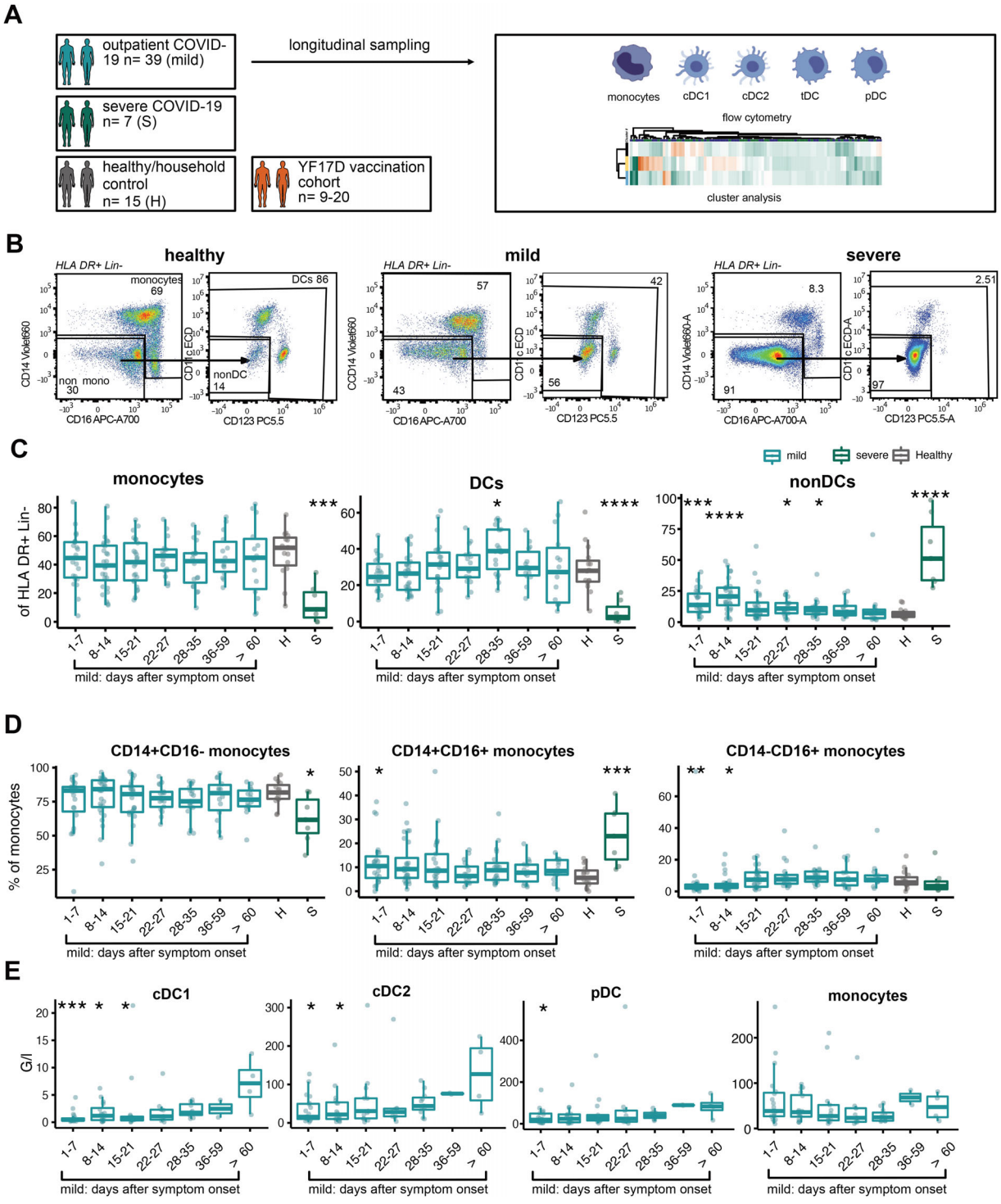

Figure 1. Time-dependent changes in the numbers of blood DC and monocyte subsets after SARS-CoV-2 infection. (A) Design of the COVID-19 study. PBMCs of outpatients with mild COVID-19, hospitalized, severe COVID-19 patients, healthy controls, and healthy donors vaccinated with YF17D were collected at multiple time points. Dendritic cell and monocyte frequencies and activation status were measured via flow cytometry. (B) Dot plot of representative healthy control, severe COVID-19 patient (12 days after infection) and mild COVID-19 patient (11 days after symptom start) showing gating of monocytes, DCs, and nonDCs within HLA DR$^+$ Lineage (CD3, 19, 20, 56, 66b) negative (Lin$^-$) living cells. (C) Monocyte, DC, and nonDC frequency within HLA DR$^+$ Lin$^-$ living cells in mild patients (blue), healthy controls (grey), and severe, hospitalized COVID-19 patients (green). Significance indicated by asterisks. (D) Frequency of monocyte subsets defined by CD14 and CD16 expression of total monocyte cells in patients with mild disease progression (blue), healthy controls (gray), and hospitalized COVID-19 patients with severe disease progression (green). (E) Absolute numbers of the indicated cell types measured in Giga per liter blood (G/l) of the patients with mild COVID-19 disease manifestations. (B–E) Significant p-values indicated by asterisks (*$p < 0.05$, **$p > 0.01$, ***$p > 0.001$, ****$p > 0.0001$) are shown as calculated in R using the Kruskal-Wallis test and Dunn's multiple testing and comparing with healthy controls (B, D) or with the last time point (E).

for the proliferation marker Ki67. The highest frequency of Ki67$^+$ cells was found in the nonDC fraction in all samples especially in those from severely affected COVID-19 patients. The frequency of Ki67$^+$ cells was also increased compared to healthy controls in pDCs, cDC2, and monocytes in patients with severe disease manifestations. In some patients with mild disease, increased Ki67 expression was seen in monocytes at later time points (Fig. 2A, B, C). A significantly increased expression of costimulatory molecule CD86 could be observed at early time points in patients with mild disease compared to healthy controls in pDC, monocytes, and nonDCs. A similar trend was observed in cDC1 and cDC2. On the contrary, in patients with severe COVID-19, downregulation of CD86 was found in monocytes, nonDCs, and cDC2, thereby showing distinct activation profiles between patients with severe and mild disease manifestations (Fig. 2D–F, gating in Fig. S2). PD-L1 expression was upregulated in cDC1 and classical monocytes of outpatients with mild disease, but a stronger upregulation was seen in patients with severe disease in all DC and monocyte subsets. While this was especially pronounced in classical monocytes, it was also observed in non-classical monocytes and pDC, cDC1, cDC2, and transitional (t)DCs. The increased expression of PD-L1 in patients with mild course of COVID-19 compared to healthy controls was also observed at late time points (up to 60 days) after symptom onset, indicating effects lasting beyond the acute phase of the disease even in mild cases (Fig. 2D, F). In some cell populations, downregulation of PD-L1 compared to healthy controls was seen, such as cDC2, tDC and nonDC. Different time courses in the expression of CD86 and PD-L1 were observed in individual patients, with a subgroup of patients expressing low levels of CD86 and high levels of PD-L1 from the earliest timepoint up to 15 days after symptom onset and another subgroup expressing lower levels of PD-L1 than the other patients at all time points (Fig. S3). Thus, a difference of activation marker expression was seen in mild compared to severe COVID-19 patients, with an upregulation of CD86 and PD-L1 detected in mild disease, and downregulation of CD86 and upregulation of PD-L1 detected in severe disease.

A subgroup of mild COVID-19 patients shows early downregulation of CD86

To investigate the different activation profiles in COVID-19 patients in an unbiased approach, dimensionality reduction was performed using principal component analysis (PCA) with all scaled and centered data obtained from flow cytometric measurements such as DC and monocyte population frequencies and their activation status. COVID-19 patients with severe disease (dark green) clearly separated from the mild cases (light blue/green and orange, color coded according to timepoint after symptom onset) in terms of PC1 and PC3 while the mild cases and healthy controls (grey) clustered together (Fig. 3A). Analysis of the PCA's rotation showed that parameters with the strongest influence on PC1 were the percentage of Ki67$^+$ pDC, the percentage of PD-L1$^+$ cells (PD-L1$^+$ cDC2, PD-L1$^+$ tDC, PD-L1$^+$ cDC1, PD-L1$^+$ pDC, PD-L1$^+$ non-classical monocytes), and the percentage of CD86$^+$ cells (CD86$^+$ intermediate monocytes, CD86$^+$ cDC2, CD86$^+$ non-classical monocytes, CD86$^+$ classical monocytes, CD86$^+$ tDC, CD86$^+$ nonDC, CD86$^+$ cDC1). Other parameters with strong influence on PC3 were the percentages of DC subsets of total DCs (DCs of HLA-DR$^+$ living, pDC of DCs, DC of HLA-DR$^+$ Lin$^-$, cDC2 of DCs, nonDC of DCs)

Subsequently, the temporal dynamics of the response within the mildly affected COVID-19 outpatients were analyzed. This analysis was restricted to 20 patients, of which longitudinal measurements with early (0 to 15 days), intermediate (16 – 30 days), and late (31 – 70 days) time points were available. The data were normalized by calculating the difference between the first and intermediate time point and between the first time point and the late time point. A positive difference (color scale: green) indicates downregulation, and a negative difference indicates upregulation (color scale: orange) at the intermediate and late time points compared to the early time point. With this normalized data k-means clustering, a centroid-based unsupervised clustering algorithm, was performed to cluster patients depending on their DC and monocyte response to SARS-CoV-2 infection. After k-means clustering of the 20 patients, cluster 1 encompassed 4 patients (median age = 54, symptoms score = 3), cluster 2 contained 13 patients (median age = 36, symptoms score = 3), and cluster 3 contained 3 patients (median age = 30, symptoms score = 2) (Fig. 3B). The greatest difference between the clusters was seen in the change of CD86 and PD-L1 expression both at the intermediate and the late time point. For example, PD-L1 expression in monocyte subsets was upregulated at the later timepoints in cluster 3, while it was downregulated or unchanged at the later time points in clusters 1 and 2 (Fig. 3D).

Patients belonging to these 3 clusters were also grouped together in a PCA analysis of the centered and scaled data (here not normalized to the first timepoint) (Fig. 3C). Especially the measurements at the earliest time point (0 to 15 days) differed between the clusters. Analysis of classical monocytes showed a CD86 downregulation and high PD-L1 expression in cluster 1, while clusters 2 and 3 contained patients with higher CD86 expression in monocytes and cluster 3 patients with very low early PD-L1 expression in monocytes (Fig. 3D). Similar effects were seen in cDC2 (Fig. 3D). The CD86 expression in cluster 1 was much lower than in the healthy control group (dotted line) and this change was still observed at later time points after symptom onset (Fig. S2). In cluster 2, CD86 expression was only decreased at late time points, thereby showing a transient and early upregulation of CD86 in these patients. On the other hand, PD-L1 expression was elevated in clusters 1 and 2 while cluster 3 showed a decreased PD-L1 expression compared to healthy controls. Cluster 1 patients showed high expression of PD-L1 and low expression of CD86 in monocytes throughout the observation period (Fig. 3D). Proliferation marker Ki67 was also differentially expressed in the clusters with a high expression of Ki67 in classical monocytes found in cluster 1, and a high expression of Ki67 in cDC2 found in cluster 1 and 3. Thus, distinct activation profiles were seen between severe hospitalized and mild outpatient COVID-19

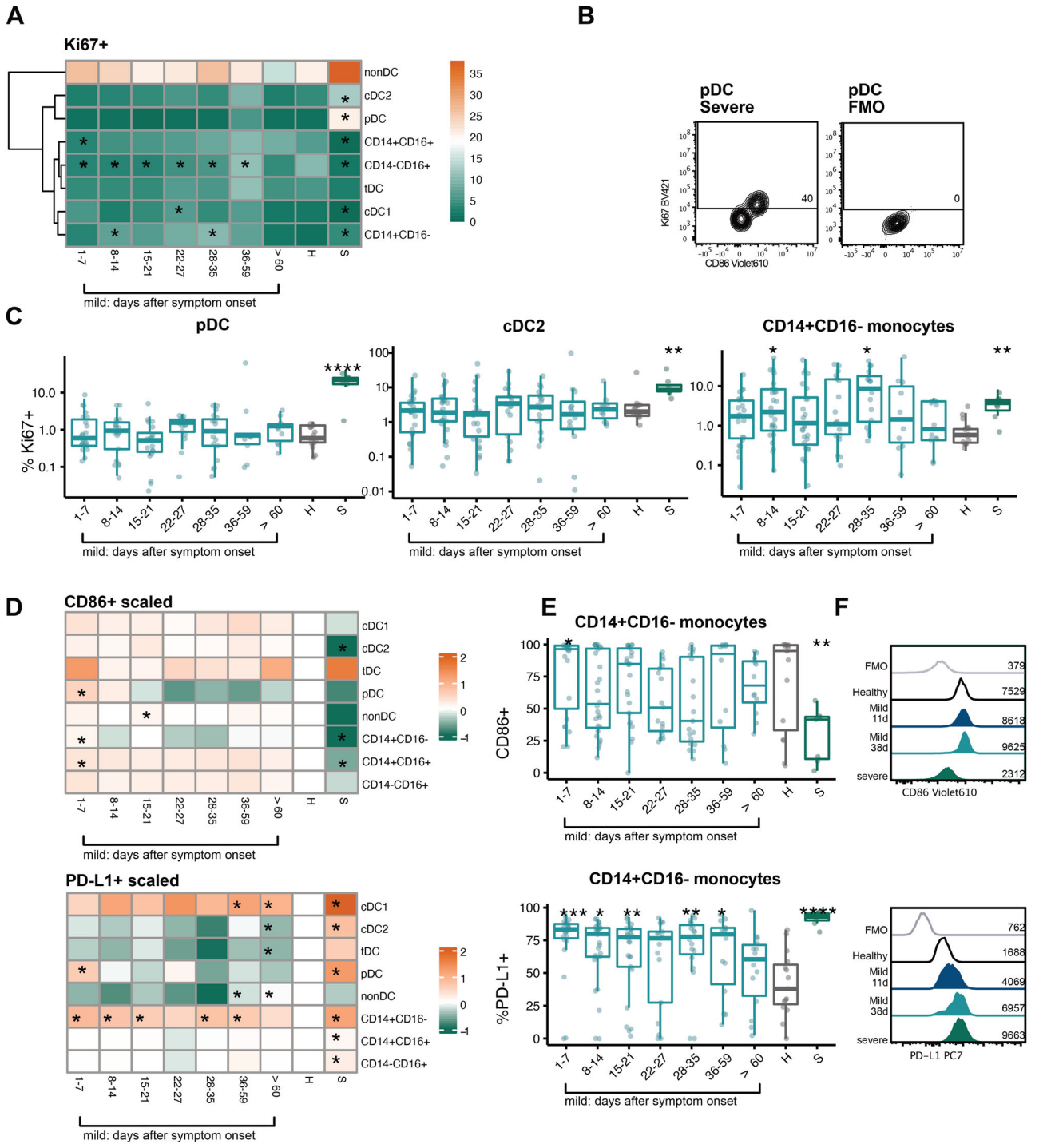

Figure 2. Activation and proliferation of DCs and monocytes in mild compared to severe COVID-19. (A) Heatmap showing the mean percentage of Ki67$^+$ cells of DC and monocyte subpopulations in patients with a mild disease progression, healthy controls (H), and hospitalized COVID-19 patients with a severe disease progression (S), unscaled. Dark orange indicates high, and green indicates low expression. (B) Representative contour plots showing Ki67 and CD86 expression in pDCs of a COVID-19 patient with severe disease progression. The FMO control for Ki67 staining is shown on the right. (C) Percentage of Ki67$^+$ pDC, cDC2, and Ki67$^+$ CD14$^+$CD16$^-$ monocytes in patients with a mild disease progression (blue), healthy controls (gray), and hospitalized COVID-19 patients with a severe disease progression (green). (D) Heatmap showing the mean percentage of CD86$^+$ and PD-L1$^+$ cells of DC and monocyte subpopulations in patients with mild disease progression, healthy controls (H), and hospitalized COVID-19 patients with a severe disease (S), scaled for each row to the healthy control. (E) Percentages of PD-L1$^+$ and CD86$^+$ CD14$^+$CD16$^-$ monocytes in mildly affected patients (blue), healthy controls (gray), and severely affected, hospitalized COVID-19 patients (green). Significant p-values are shown as calculated in R using the Kruskal–Wallis test and Dunn's multiple testing and comparing with healthy control. Significance is indicated by asterisks (*$p < 0.05$, **$p > 0.01$, ***$p > 0.001$, ****$p > 0.0001$). (F) Representative histograms of PD-L1 and CD86 expression in classical monocytes of a healthy donor and a COVID-19 patient with mild symptoms at 11 and 38 days after symptom onset. Numbers indicate mean fluorescence intensity (MFI) values.

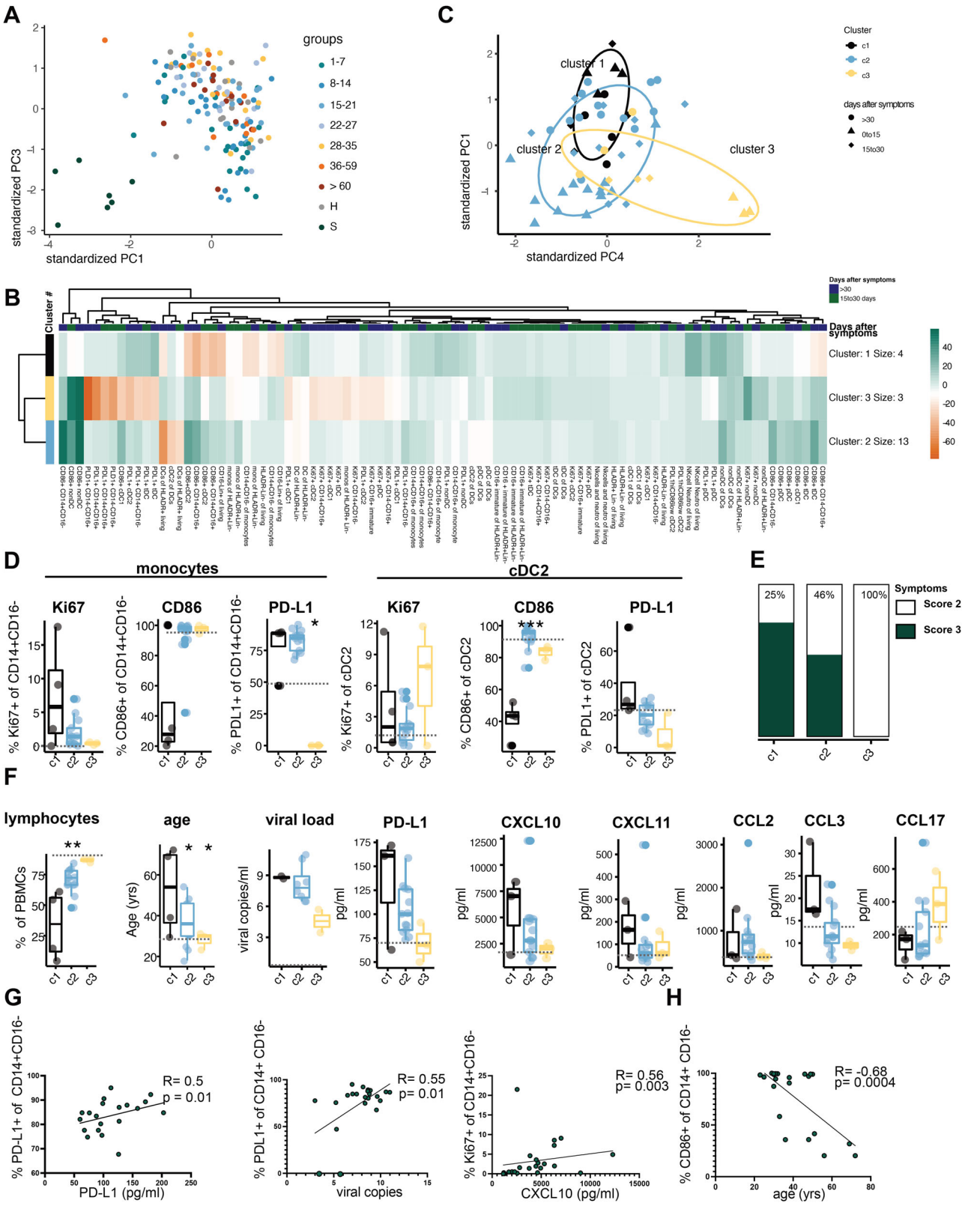

Figure 3. Clustering of COVID-19 patients by DC and monocyte features. (A) PCA analysis of all mild (time after symptom onset indicated by different blue and orange colors), severe (dark green, median 5 days after diagnosis), and healthy donors (grey). The parameters shown in the heatmap in (B) were used for the PCA. (B and C) 20 patients with mild disease that had been sampled on three consecutive time points were selected. Longitudinal measurements were grouped into three timepoints, 0–15 days after symptom onset, 16–30 days after symptom onset, and over 30 days after symptom onset. (B) Heatmap showing k means clustering analysis of the differences between the measurements from the early

cases. Additionally, within the outpatient cohort distinct activation profiles were observed as well.

Low expression of CD86 in monocytes is associated with higher age and more symptomatic disease

In cluster 1, a clinical score of 3 was reached in three of four patients (75%). In cluster 2, a clinical score of 2 was assigned to six patients (46%) and a score of 3 was reached by seven patients (54%), whereas all patients in cluster 3 had a score of 2 (Fig. 3E). Patients in cluster 1 also showed a very low percentage of lymphocytes at the early time point (Fig. 3F), consistent with a correlation of lymphopenia with higher disease severity that has been described [17]. Patients in cluster 1 were also older than in clusters 2 and 3 (median age 54 vs 36 and 30). Viral copy numbers in nasopharyngeal swabs in the first week after symptom onset tended to be higher in the more symptomatic patients in clusters 1 and 2 at this time point (Fig. 3F, median copies 9 vs 8 and 5).

Our cluster analysis indicated that higher age coinciding with more symptomatic disease and lymphopenia was associated with changes in the expression of activation marker CD86. The described phenotypic changes in blood DCs and monocytes could be due to the systemic inflammatory response with elevated cytokine and chemokine levels in the blood. We therefore analyzed the concentrations of cytokines and plasma proteins at the early time point (day 1–15 after symptom onset) in the three clusters and detected higher levels of plasma PD-L1 in cluster 1 and 2 compared to cluster 3 consistent with higher expression of PD-L1 in monocytes and DCs in these patient clusters (Fig. 3F). Plasma levels of C-X-C motif chemokine ligand (CXCL)10, CXCL11, CC-chemokine ligand (CCL)2 and CCL3 were highly variable but all patients with chemokine levels above those of healthy controls at this time point belonged to cluster 1 and 2, which contain the patients with more pronounced symptoms and higher age (as shown in Fig. 3F). CCL17 concentrations showed a tendency to be lower in cluster 1 patients. Plasma PD-L1 levels positively correlated with PD-L1 expression on monocytes (Fig. 3G) confirming the flow cytometric measurements. Interestingly, PD-L1 expression on monocytes also significantly correlated with viral load (Fig. 3G). The activation marker expression of CD86 and PD-L1 did not correlate significantly with any of the cytokines and plasma proteins measured. However, Ki67 expression in classical monocytes significantly correlated with CXCL10 (Fig. 3G). The percentages of $CD86^+$ classical monocytes and cDC2 at the first measured time point were inversely correlated with age in the COVID-19 outpatient cohort (classical monocytes: $R = -0.68$, $p = 0.0004$; cDC2: $R = -0.53$, $p = 0.009$), but not in the healthy control group (classical monocytes: $R = -0.13$, $p = 0.97$; cDC2: $R = -0.03$, $p = 0.9$;) (Fig. 3H; Fig. S3).

Taken together, the unbiased clustering analysis reveals variability in the innate immune response within the group of mild COVID-19 patients. A higher clinical score in mild COVID-19 patients was associated with higher age, viral load, and PD-L1 expression as well as lower lymphocyte count and CD86 expression. However, the majority of mild COVID-19 patients had a low clinical score and showed high expression of both PD-L1 and CD86.

Circulating cDCs are transiently activated and proliferate in response to YF17D vaccination

In order to put the observed response of circulating DCs to SARS-CoV-2 infection into context with a well-characterized antiviral immune response leading to long-lasting protection, YF17D vaccination was used as a model of such a coordinated and efficient immune response to viral infection in humans. Healthy volunteers were vaccinated with YF17D and blood was drawn at day 0 before vaccination, and days 3, 7, 14, and 28 after vaccination and PBMCs were analyzed via flow cytometry (Fig. 4A). Similar to infection with SARS-CoV-2, early expansion of intermediate monocytes could be seen (Fig. 4B). In contrast to our observations in SARS-CoV-2 infected patients with mild or severe disease no expansion of nonDCs, immature $HLA\text{-}DR^+$ Lin- cells lacking typical monocyte and DC markers, was detected after yellow fever vaccination (Fig. 4C). In the DC fraction a significant expansion of pDCs was seen 3 days after vaccination followed by a reduction compared to baseline on day 14 after vaccination, whereas pDC frequency was rather reduced at early time points after SARS-CoV-2 infection (Fig. 4D). Increased proliferation of pDCs was not detected after vaccination (Fig. 4F). The percentages of cDC1 and cDC2 were concomitantly slightly reduced on day 3 and day 7 after YF17D vaccination (statistically significant only for cDC2 on day 3) and returned to baseline afterward (Fig. 4D). This recovery was preceded by a temporary increase in the percentage of proliferating $Ki67^+$ cDCs on days 3 and 7 after vaccination indicating increased turnover and subsequent rapid regeneration of the circulating cDC compartment (Fig. 4F). Unlike in patients with COVID-19 no significant reduction of pDC and cDC1 counts

to the intermediate and to the late time point within the same patients calculated by subtracting the values of the intermediate and late time point from the values of the early time point. (C) PCA analysis of scaled and centered data from parameters shown in B without normalization to first timepoint. Distinction of k means clusters by color (black: cluster 1, blue: cluster 2, yellow: cluster 3) and time after symptom onset by symbol (round > 30 days, triangle = 0–15 days, diamonds = 15–30 days). (D) Percentage of $Ki67^+$, $CD86^+$, and $PD\text{-}L1^+$ $CD14^+CD16^-$ monocytes and cDC2 of patients with mild COVID-19 as divided by cluster identity. Dotted line indicates healthy controls. (E) Clinical score and (F) age, percentage of lymphocytes of total PBMCs, nasopharyngeal viral load as viral copies, and serum concentrations of the indicated soluble mediators (PD-L1, CXCL10, CXCL11, CCL2, CCL3, CCL17) of the patients in the 3 clusters at the earliest timepoint after symptom onset. Dotted line indicates healthy controls. (G) Spearman correlation of the serum concentration of PD-L1 with the percentage of $PD\text{-}L1^+$ $CD14^+$ $CD16^-$ monocytes and with viral copies; Measurements at the earliest time points were used for the analysis. (H) Spearman correlation analysis of the outpatient cohort using the first measured timepoint after symptom onset (<7 days) of $CD86^+$ $CD14^+CD16^-$ monocytes with age. R values and p values indicated.

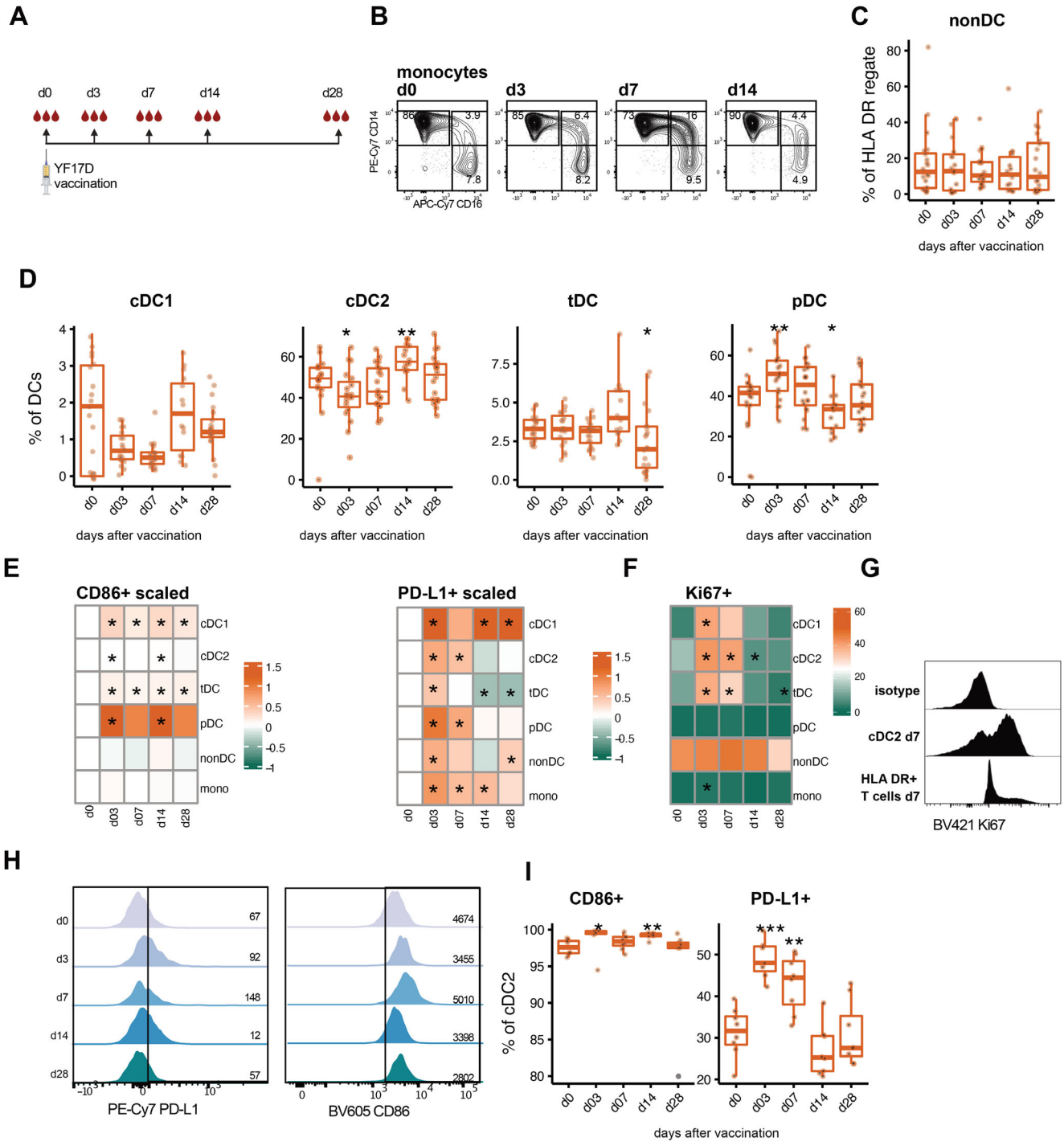

Figure 4. Coordinated response of circulating DCs and monocytes to YF vaccination. (A) Design of the YF17D vaccination study. Blood was drawn on day 0 before and days 3, 7, 14, and 28 after vaccination with YF17D. (B) Contour plot showing monocyte population frequencies on d0, 3, 7, and 14 after vaccination in one representative donor. (C) Percentage of nonDCs of HLA DR gate before and after vaccination with YF17D. (D) Changes of frequencies of pDCs and cDC2 of total DCs before and after vaccination with YF17D ($n = 20$). (E) Heatmap showing Log2 fold changes of percentage of CD86$^+$ and PD-L1$^+$ cells to day 0 control over time after vaccination. Orange color indicates increase, green decrease of CD86$^+$ and PD-L1$^+$ cells compared to d0 percentages ($n = 9$). (F) Heatmap showing percentages of Ki67$^+$ cells over time after vaccination ($n = 9$). (G) Histograms showing representative expression of Ki67 in cDC2 and HLA DR$^+$ T cells on day 7 after vaccination, compared to the isotype control. (H) Histograms showing representative expression of CD86 and PD-L1 in cDC2 before and after vaccination with YF17D scaled to d0. Numbers indicate mean fluorescence intensity (MFI) values. (I) Boxplots showing percentage of CD86$^+$ and PD-L1$^+$ cells before and after vaccination in cDC2 ($n = 9$).

was seen in the peripheral blood of YF17D vaccinated subjects at any of the timepoints (Fig. S4). cDC2 and tDC counts were significantly reduced on day 7 after vaccination. However, the decrease of DC counts on day 7 was only to 60% of baseline in the YF17D vaccinees compared to 28% of baseline in patients with mild COVID-19 in cDC2, and only 61% compared to 41% in tDCs. Thereby, in YF17D the reduction of cDC2 and tDCs was not as pronounced as in COVID-19 and not as long-lasting.

Activation markers CD86 and PD-L1 were both temporarily upregulated in DC and monocyte subsets after vaccination with YF17D (Fig. 4E). PD-L1 and CD86 were also upregulated in the majority of SARS-CoV-2 infected outpatients compared to healthy controls except for a subgroup of older SARS-CoV-2 infected outpatients and patients with severe COVID-19 that showed reduced CD86 expression (shown in Figs. 2D and 3D). Age might contribute to differences observed between the response to SARS-CoV-2 and YF17D vaccination because the vaccination cohort was younger. We therefore restricted the analysis to a subgroup of the outpatient COVID-19 cohort below the age of 35 (COVID-19: median age 30, $n = 11$; healthy: median age = 25, $n = 9$). In this subgroup of younger patients, we also detected an increased percentage of nonDCs in HLADR$^+$ Lin$^-$ cells, a reduced frequency of CD14$^-$CD16$^+$ non-classical monocytes and a tendency towards increased PD-L1 and CD86 expression in monocytes at the first timepoint after diagnosis as shown for the whole cohort (Fig. S5A-C). Also, in the younger subgroup of COVID-19 patients a longer lasting reduction of DC subset counts without increased frequency of proliferating DCs was observed (Fig. S5D–F).

Thus, YF17D vaccination induced a transient coordinated response of circulating antigen-presenting cells (APCs) with the peak on day 7 after vaccination and rapid recovery of blood cDCs, while the responses in COVID-19 were longer-lasting even in mild outpatient cases and led to incongruent regulation of CD86 and PD-L1 in monocytes and cDCs in a subgroup of older patients with mild, but symptomatic disease.

Discussion

In this study, the innate immune response of peripheral blood DCs and monocytes of non-hospitalized patients diagnosed with COVID-19 was characterized and compared to the response in hospitalized COVID-19 patients, healthy controls, and individuals vaccinated with YF17D. The study cohort presented here differs from previous COVID-19 study cohorts since it includes not only hospitalized patients with severe COVID-19 disease manifestations but also a large cohort of patients with only mild symptoms that were self-isolating at home and that were regularly followed up over a long time period. These patients lacked major comorbidities and therapeutic interventions that are often found in cohorts of hospitalized patients with COVID-19 and can limit the interpretation of the study data.

Interestingly, many changes found in patients with severe disease progression after SARS-CoV-2 infection were also identified in the non-hospitalized patients albeit to a lower extent. Several reports have described a reduction in monocyte and DC numbers in the peripheral blood of patients with severe COVID-19 [10, 11, 13–15, 18, 19]. We could confirm the persistent reduction in DC subset numbers in patients with mild disease progression. Perez-Gomez *et al.* also reported a long-lasting reduction of cDC2 and pDCs in the blood of hospitalized and non-hospitalized patients alike [18]. Thus, depletion of DCs from the blood which may be due to increased extravasation and/or increased cell death also occurs in mild disease. An increased frequency of proliferating HLA DR$^+$ CD86$^{+/-}$ cells lacking markers of differentiated DCs, monocyte, and other cell lineages (B, T, NK, granulocyte) previously described by us in hospitalized COVID-19 patients with severe disease [14] was also found in the peripheral blood of patients with mild COVID-19 although less pronounced than in severe COVID-19. The expansion of this population is therefore a consequence of the acute SARS-CoV-2 infection and not due to comorbidities, medications, or severe illness. The high percentage of Ki67$^+$ cells in this population at all timepoints during the disease could indicate a progenitor function. But, in our previous study [14], where we found these non-DCs to be expanded in hospitalized COVID-19 patients, expression of CD34, CD117, CD115, or CD127 was not detected and their phenotype didn't match that of known progenitor populations of monocytes/macrophages, DCs, and lymphoid cells. A similar increase in HLA-DR$^+$ immature cells with a concomitant decrease of DC subsets in the blood was previously observed in malaria patients [20, 21]. The "non-DCs" found in both severe and mild COVID-19 patients could be non-canonical DC-like cells or precursors generated in an attempt to regenerate the DC compartment. Since the same population was not found to be increased after vaccination with YF17D, it may be an indicator of the emergency myelopoiesis and systemic inflammation known to occur during acute SARS-CoV2 infection [13, 22].

Within the monocyte compartment, a shift toward intermediate monocytes and a reduction of non-classical monocytes were observed at early time points in COVID-19 patients with mild disease confirming findings in hospitalized patients with more severe disease [13, 16]. The transiently increased frequency of intermediate monocytes that was also seen after YF17D vaccination is a common feature of the systemic response to viral infection and vaccination [9, 23–25] whereas the reduction in non-classical monocytes is rather specific for SARS-CoV-2 infection [13, 16, 26].

We had previously observed reduced CD86 and increased PD-L1 expression in circulating cDCs and monocytes in a cohort of hospitalized COVID-19 patients that coincided with a reduced capacity of these APCs to stimulate T cells [14]. In contrast, the majority of patients in our outpatient cohort showed a high CD86 expression early on which was reduced at later time points suggesting initial upregulation followed by return to or below baseline. However, reduced expression of co-stimulatory molecule CD86 on cDCs and monocytes was detected in a cluster of patients with the highest clinical score and the lowest lymphocyte count. In the outpatient cohort, we also found an inverse correlation of monocyte CD86 expression with age that was not seen in healthy

donors. Thus, low CD86 expression in circulating DCs and monocytes is a feature associated with more symptomatic disease and higher age even in a cohort of outpatients with a favorable course of disease in the absence of confounding factors such as major comorbidities and therapeutic interventions.

Multiple studies have described the association of higher age with more severe COVID-19 disease outcomes [27]. Age-associated changes in the immune response such as altered cytokine responses in elderly patients have been shown to contribute to more severe COVID-19 [28]. Interestingly, in aged mice, upregulation of CD86 is reduced after TLR2 and influenza-induced stimulation [29]. Monocytes from elderly people respond to stimulation by reduced production of cytokines [30] and reduced upregulation of CD80 [31]. Thereby, reduced or altered ability to respond to certain viral and non-viral stimuli seems to be a conserved effect in aged mice and humans. In patients with COVID-19, the age-dependent downregulation of CD86 expression in APCs could influence activation of subsequent adaptive immune responses.

PD-L1 expression in classical monocytes was persistently increased in the majority of patients in our outpatient cohort with the exception of a few younger patients with less severe symptoms, lower viral load and normal levels of inflammatory chemokines. Our study indicates that CD86 and PD-L1 expression in monocytes and DCs stratify patients according to disease intensity. Soluble (s)PD-L1 levels correlated with PD-L1 expression in monocytes in our study. Higher levels of sPD-L1 were found in COVID-19 patients requiring mechanical ventilation compared to those not requiring mechanical ventilation [32]. PD-L1 expression can be induced by type I IFNs as well as by IFN-γ produced by natural killer cells and T cells during viral infection [33].

Vaccination with the live-attenuated viral vaccine YF17D is accompanied by temporary changes in gene expression, frequency, and phenotype of circulating immune cells including DCs and monocytes indicating a coordinated and reversible systemic innate response that is relevant for the high efficacy of this viral vaccine [7, 34]. Here we show that there are common features as well as substantial differences in the response of circulating DC and monocyte to SARS-CoV-2 infection compared to YF17D vaccination. In contrast to the longer lasting reduction in cDCs and pDCs observed after SARS-CoV-2 infection, which occurred also in the younger patients, there was only a temporary and minor decrease in cDC2 after YF17D vaccination, followed by rapid replenishment. An increase in the percentage of $Ki67^+$ cDCs preceded the recovery of the blood cDC compartment suggesting that active proliferation of cDCs or release of recently generated proliferating cDCs into the circulation rapidly compensate the loss of cDCs in the response to YF17D vaccination. This greatly enhanced proliferative response in cDCs was not seen in COVID-19 outpatients despite the reduction in cDC numbers indicating impaired or delayed regeneration. Similarly, the reduction in circulating pDCs that was only seen after SARS-CoV-2 infection was not accompanied by increased proliferation in mild COVID-19. These differences between the response to YF17D vaccination and SARS-CoV2 infection were probably not due to the younger age of the vaccinees, as reduction in DC numbers without remarkable proliferation was also observed in younger patients. Increased proliferation of cDCs and pDCs could however be detected in severe COVID-19 patients, which can be interpreted as an attempt to replenish the DC compartment in reaction to the profound depletion seen in these cases. The dysregulated "emergency" myelopoiesis with expansion of immature neutrophils and monocytes observed in COVID-19 patients [13] as well as increased cell death in DCs [35] could be responsible for the delayed recovery of the DC compartment. In mouse models of bacterial and viral infection development of cDCs from precursors was also shown to be reduced while monopoiesis was increased [36, 37].

In the majority of SARS-CoV-2 infected outpatients with mild disease, a similar response of blood monocytes and cDCs with temporary upregulation of CD86 and PD-L1 expression was observed after YF17D vaccination indicating a "normal" controlled response to infection. A similar activation of cDC2 and monocytes was also seen after adenoviral vaccination [38]. Nevertheless, a subgroup of COVID-19 outpatients showed reduced CD86 and high PD-L1 expression in monocytes and cDC2s, a phenotype associated with reduced ability to stimulate T cells that was seen also in hospitalized patients with more severe disease (current study and [13, 14, 39]. This indicates a functional impairment of antigen-presenting cells in a minor fraction of SARS-COV-2 infected outpatients while in the majority of oligosymptomatic patients the DC and monocyte phenotypes were comparable to those detected after YF17D vaccination, which leads to highly efficient T cell activation [7, 40, 41].

The in-depth characterization of the response of circulating DC and monocyte subpopulations to viral infection and vaccination presented here defines key features of innate immune responses leading to protective immunity as well as indicators of dysregulated responses of antigen-presenting cells to SARS-CoV-2 infection that may also occur in a subgroup of outpatients in the absence of comorbidities, very old age, severe illness, and specific therapies.

Materials and methods

COVID-19 study participants

Patients were recruited as part of the KoCo19 study by providing information and contact details to households of Munich with at least one registered positive polymerase chain reaction (PCR) test for SARS-CoV-2 reported to the Health Department of Munich. For this longitudinal cohort, which has been described in detail by Puchinger et al. [42], PCR-positive individuals and their respective household members were enrolled, and blood samples were collected in the Division of Infectious Diseases and Tropical Medicine, University Hospital, LMU, Munich, Germany between May 2020 and February 2021 at defined timepoints after primary diagnosis during household visits or at a

central testing facility with approval from the LMU ethics committee (no. 20–371) [42]. The time of symptom onset and the symptom intensity as well as preexisting conditions and the use of medications were documented (self-reported using a questionnaire, Table S1). One asymptomatic patient was excluded from the analysis since day after symptom onset could not be calculated. In addition, blood samples from patients with severe COVID-19 collected in September 2020 were analyzed (COVID-19 Registry of the LMU University Hospital Munich with approval from the LMU ethics committee (no. 20–24 and 592-16, CORKUM, WHO trial ID DRKS00021225)). Patients were assigned a maximal clinical score that was adapted from the WHO ordinal scale (WHO COVID-19 Therapeutic Trial Synopsis available online: https://www.who.int/publications/i/item/covid-19-therapeutic-trial-synopsis): score 1: asymptomatic; score 2: mild symptoms, not hospitalized; score 3: moderate symptoms, not hospitalized; score 4: oxygen by mask or nasal tube; 5: non-invasive ventilation; 6: invasive ventilation; 7: organ support (extracorporeal membrane oxygenation); 8: death (patients with scores 4–8 were hospitalized).

YF17D vaccination cohort

PBMC from YF17D vaccinees were obtained from a subgroup of a larger vaccination cohort at the Division of Infectious Diseases and Tropical Medicine and the Department of Clinical Pharmacology (Prof. Dr, Simon Rothenfusser), University Hospital, LMU Munich, Germany). The study was approved by the LMU ethics committee no. 86-16. All participants were healthy (aged 21 to 35 years, Table S2) and had not been previously exposed to wild-type YFV, and were not previously immunized against YF. After giving informed consent, the patients received a single subcutaneous injection of the YF17D vaccine (Stamaril, Sanofi Pasteur, Lyon, France) at the Division of Infectious Diseases and Tropical Medicine at LMU Munich. Blood was drawn directly before vaccination and on days 3, 7, 14, and 28 after vaccination using the S-Monovette Sodium-Heparin (Sarstedt, Nürnbrecht, Germany).

PBMC isolation and flow cytometry

PBMCs were isolated from whole blood by gradient centrifugation and directly used for flow cytometric analysis. PBMC from COVID-19 patients and healthy controls were stained and analyzed together on the day of sampling. PBMC were stained in 200 μl of PBS, 2mM EDTA, 10% FCS (v/v) with fluorescently labeled antibodies as indicated in the supplementary Table S3 and incubated for 20 min at room temperature. Fixable viability dyes were used according to the manufacturer's protocol. Cells were fixed and permeabilized with FoxP3/transcription factor staining buffer (ThermoFisher, Cat. # 00-5523-00) following the manufacturer's instructions. Intracellular staining for Ki67 was performed and fixed afterward with Cellfix (BD, cat. # 340181) following the manufacturer's instructions. Samples were measured using the CytoFLEX S flow cytometer (Beckman Coulter). FCS files were exported and analyzed with FlowJo software v10.7.1. Data were analyzed in a blinded fashion and fluorescence minus one controls for PD-L1, CD86, and Ki67 were used. Samples with population counts <10 cells were excluded. To obtain lymphocyte and monocyte cell counts per μl blood a BD Multitest 6-color TBNK test (BD cat # 337166) was performed: In the KoCo-Immu study, fresh EDTA whole blood samples were drawn at all visits and were stained according to the manufacturer's instructions and measured on a CytoFLEX S cytometer. The absolute number of monocyte and DC subsets were calculated from these cell counts.

Plasma analytes

The concentrations of the indicated cytokines and PD-L1 were analyzed in plasma samples from patients enrolled in the COVID-19 study by 26 plex human magnetic Luminex assay (R & D Systems, cat. # LXSAHM-26) according to the manufacturer's instructions and analyzed by MAGPX13263702 (Luminex).

Data analysis

Statistical analysis was performed using GraphPad Prism 9.1.0 and R 4.0.3 (packages used:ggplot2_3.3.3, ComplexHeatmap_2.4.3, ggstatsplot_0.6.8). PCA was performed using the parameters shown in the heatmap in Fig. 3B from all timepoints measured without normalizing to first timepoint. Statistics were tested with the Kruskal-Wallis test. Multiple testing was corrected using the Dunn's multiple comparison test. Box plots show the upper and lower quartiles, and whiskers indicate 1.5 IQR. Subpopulations containing less than 10 cells were excluded from analysis. *p*-Values below 0.05 were considered to indicate statistically significant differences.

Acknowledgments: This work is part of the theses of Elena Winheim and Tabea Eser. We thank Claudia Bräu-Heberger, Sabine Rappe, and Yvonne Schäfer for technical support. We acknowledge the Core Facility Flow Cytometry of the Biomedical Center, LMU Munich, and thank Lisa Richter and Pardis Khosravani. This work was funded by the Deutsche Forschungsgemeinschaft (DFG) project no. 458597554, SEPAN to C.G. and M.H. (GE 2128/3-1 and HO 2228/12-1), project no. 210592381 SFB1054-TPA06 to A.B.K., project no. 369799452 TRR237-TPB14 to A.B.K. and S.R., project no. 391217598 to A.B.K. and S.R. C.G. received funding from the Bavarian State Ministry of Science and Art (Langfristige Nachverfolgung der zellulären und humoralen Immunantwort nach SARS-CoV-2-Infektion und Impfung 2021; Corona Forschungsprogramm 2021/2022). The KoCo19 project is funded by the Bavarian State Ministry of Science and Art,

the LMU Klinikum München, and Helmholtz Zentrum München. A.K. received funding from the Bavarian State Ministry of Science and the Arts (Corona Forschungsprogramm 2021 and 2022). E.W. received a scholarship from the Villigst Foundation. The CORKUM study was supported by LMUexcellent, funded by the Federal Ministry of Education and Research (BMBF) and the Free State of Bavaria under the Excellence Strategy of the Federal Government and the Länder. The funding bodies do not play a role in the design of the study and collection, analysis, nor in interpretation of data or in writing the manuscript.
Open access funding enabled and organized by Projekt DEAL.

Conflict of interest disclosure: Clemens Scherer received speaker honoraria from AstraZeneca (not connected to the submitted work). The other authors declare no commercial or financial conflict of interest.

Ethics approval statement: All studies were conducted with approval from the ethics committee of the LMU Munich.

Patient consent statement: Informed consent was obtained from all included patients and donors.

Author contributions: C.G., M.H., A.B.K., E.W., T.E., and S.R. conceptualized the study. E.W., T.E., L.Ri., F.D., M.A., O.B. A.S., H.K., and M.P. performed investigations. E.W. and T.E. performed formal analysis. E.W., T.E., L.Ri., and K.E. perpared the methodology. C.S., J.C.H., M.M., and M.B-B. acquired resources. A.B.K., C.G., S.R., and M.H. supervised the study. A.B.K., C.G., M.H., S.R., and M.B-B. acquired funding. E.W. visualized the study. E.W. and A.B.K. wrote the original draft. E.W., A.B.K., C.G., and S.R. reviewed and edited the final manuscript.

Data availability statement: The data that support the findings of this study are available from the corresponding author upon reasonable request.

Peer review: The peer review history for this article is available at https://publons.com/publon/10.1002/eji.202250090

References

1 **Zhang, J. -J., Dong, X., Liu, G. -H. and Gao, Y. -D.**, Risk and Protective Factors for COVID-19 Morbidity, Severity, and Mortality. *Clinical Reviews in Allergy & Immunology*. 2022. **9**: 1–18.

2 **Peyneau, M., Granger, V., Wicky, P. H., Khelifi-Touhami, D., Timsit, J. F., Lescure, F. X., Yazdanpanah, Y. et al.**, Innate immune deficiencies are associated with severity and poor prognosis in patients with COVID-19. *Sci. Rep.* 2022. **12**(1): 638.

3 **Diamond, M. S. and Kanneganti, T. D.**, Innate immunity: the first line of defense against SARS-CoV-2. *Nat. Immunol.* 2022. **23**(2): 165–176.

4 **Lim, H. K., Huang, S. X. L., Chen, J., Kerner, G., Gilliaux, O., Bastard, P., Dobbs, K. et al.**, Severe influenza pneumonitis in children with inherited TLR3 deficiency. *J. Exp. Med.* 2019. **216**(9): 2038–2056.

5 **Galeas-Pena, M., McLaughlin, N. and Pociask, D.**, The role of the innate immune system on pulmonary infections. *Biol. Chem.* 2019. **400**(4): 443–456.

6 **Hernandez, N., Bucciol, G., Moens, L., Le Pen, J., Shahrooei, M., Goudouris, E., Shirkani, A. et al.**, Inherited IFNAR1 deficiency in otherwise healthy patients with adverse reaction to measles and yellow fever live vaccines. *J. Exp. Med.* 2019. **216**(9): 2057–2070.

7 **Querec, T. D., Akondy, R. S., Lee, E. K., Cao, W., Nakaya, H. I., Teuwen, D., Kim, A. P. et al.**, Systems biology approach predicts immunogenicity of the yellow fever vaccine in humans. *Nat. Immunol.* 2009. **10**(1): 116–125.

8 **Pulendran, B.**, Learning immunology from the yellow fever vaccine: innate immunity to systems vaccinology. *Nat. Rev. Immunol.* 2009. **9**(10): 741–747.

9 **Arunachalam, P. S., Scott, M. K. D., Hagan, T., Li, C., Feng, Y., Wimmers, F., Grigoryan, L. et al.**, Systems vaccinology of the BNT162b2 mRNA vaccine in humans. *Nature.* 2021. **596**(7872): 410–416.

10 **Arunachalam, P. S., Wimmers, F., Mok, C. K. P., Perera, R., Scott, M., Hagan, T., Sigal, N. et al.**, Systems biological assessment of immunity to mild versus severe COVID-19 infection in humans. *Science.* 2020. **369**(6508): 1210–1220.

11 **Kvedaraite, E., Hertwig, L., Sinha, I., Ponzetta, A., Hed Myrberg, I., Lourda, M., Dzidic, M. et al.**, Major alterations in the mononuclear phagocyte landscape associated with COVID-19 severity. *Proc. Natl. Acad. Sci. U S A.* 2021. **118**(6): e2018587118.

12 **Saichi, M., Ladjemi, M. Z., Korniotis, S., Rousseau, C., Ait Hamou, Z., Massenet-Regad, L., Amblard, E. et al.**, Single-cell RNA sequencing of blood antigen-presenting cells in severe COVID-19 reveals multi-process defects in antiviral immunity. *Nat. Cell Biol.* 2021. **23**(5): 538–551.

13 **Schulte-Schrepping, J., Reusch, N., Paclik, D., Baßler, K., Schlickeiser, S., Zhang, B., Krämer, B. et al.**, Severe COVID-19 is marked by a dysregulated myeloid cell compartment. *Cell.* 2020. **182**: 1419–1440.

14 **Winheim, E., Rinke, L., Lutz, K., Reischer, A., Leutbecher, A., Wolfram, L., Rausch, L. et al.**, Impaired function and delayed regeneration of dendritic cells in COVID-19. *PLOS Pathogens.* 2021. **17**(10): e1009742.

15 **Zhou, R., To, K. K., Wong, Y. C., Liu, L., Zhou, B., Li, X., Huang, H. et al.**, Acute SARS-CoV-2 Infection Impairs Dendritic Cell and T Cell Responses. *Immunity.* 2020. **53**(4): 864-877. e5.

16 **Silvin, A., Chapuis, N., Dunsmore, G., Goubet, A. G., Dubuisson, A., Derosa, L., Almire, C. et al.**, Elevated Calprotectin and Abnormal Myeloid Cell Subsets Discriminate Severe from Mild COVID-19. *Cell.* 2020. **182**(6): 1401-1418. e18.

17 **Zhou, F., Yu, T., Du, R., Fan, G., Liu, Y., Liu, Z., Xiang, J. et al.**, Clinical course and risk factors for mortality of adult inpatients with COVID-19 in Wuhan, China: a retrospective cohort study. *Lancet.* 2020. **395**(10229): 1054–1062.

18 **Perez-Gomez, A., Vitalle, J., Gasca-Capote, C., Gutierrez-Valencia, A., Trujillo-Rodriguez, M., Serna-Gallego, A., Muñoz-Muela, E. et al.**, Dendritic cell deficiencies persist seven months after SARS-CoV-2 infection. *Cell Mol. Immunol.* 2021. **18**(9): 2128–2139.

19 **Sanchez-Cerrillo, I., Landete, P., Aldave, B., Sanchez-Alonso, S., Sanchez-Azofra, A., Marcos-Jimenez, A., Ávalos, E. et al.**, COVID-19 severity associates with pulmonary redistribution of CD1c+ DCs and inflammatory transitional and nonclassical monocytes. *J. Clin. Invest.* 2020. **130**(12): 6290–6300.

20 **Pinzon-Charry, A., Ho, C. S., Laherty, R., Maxwell, T., Walker, D., Gardiner, R. A., O'Connor, L. et al.**, A population of HLA-DR+ immature cells accumulates in the blood dendritic cell compartment of patients with different types of cancer. *Neoplasia.* 2005. **7**(12): 1112–1122.

21 **Pinzon-Charry, A., Woodberry, T., Kienzle, V., McPhun, V., Minigo, G., Lampah, D. A., Kenangalem, E. et al.**, Apoptosis and dysfunction of blood dendritic cells in patients with falciparum and vivax malaria. *J. Exp. Med.* 2013. **210**(8): 1635–1646.

22 **Wilk, A. J., Lee, M. J., Wei, B., Parks, B., Pi, R., Martínez-Colón, G. J., Ranganath, T. et al.**, Multi-omic profiling reveals widespread dysregulation of innate immunity and hematopoiesis in COVID-19. *J. Exp. Med.* 2021. **218**(8): e20210582.

23 **Kwissa, M., Nakaya, H. I., Onlamoon, N., Wrammert, J., Villinger, F., Perng, G. C., Yoksan, S. et al.**, Dengue virus infection induces expansion of a CD14(+)CD16(+) monocyte population that stimulates plasmablast differentiation. *Cell Host. Microbe.* 2014. **16**(1): 115–127.

24 **Martins, M. A., Silva, M. L., Eloi-Santos, S. M., Ribeiro, J. G., Peruhype-Magalhaes, V., Marciano, A. P., Homma, A. et al.**, Innate immunity phenotypic features point toward simultaneous raise of activation and modulation events following 17DD live attenuated yellow fever first-time vaccination. *Vaccine.* 2008. **26**(9): 1173–1184.

25 **Michlmayr, D., Andrade, P., Gonzalez, K., Balmaseda, A. and Harris, E.**, CD14+ CD16+ monocytes are the main target of Zika virus infection in peripheral blood mononuclear cells in a paediatric study in Nicaragua. *Nat. Microbiol.* 2017. **2**(11): 1462–1470.

26 **Mueller, K. A. L., Langnau, C., Günter, M., Pöschel, S., Gekeler, S., Petersen-Uribe, Á., Kreisselmeier, K. P. et al.**, Numbers and phenotype of nonclassical CD14dimCD16+ monocytes are predictors of adverse clinical outcome in patients with coronary artery disease and severe SARS-CoV-2 infection. *Cardiovasc. Res.* 2021. **117**(1): 224–239.

27 **O'Driscoll, M., Ribeiro Dos Santos, G., Wang, L., Cummings, D. A. T., Azman, A. S., Paireau, J., Fontanet, A. et al.**, Age-specific mortality and immunity patterns of SARS-CoV-2. *Nature.* 2021. **590**(7844): 140–145.

28 **Pirabe, A., Heber, S., Schrottmaier, W. C., Schmuckenschlager, A., Treiber, S., Pereyra, D., Santol, J. et al.**, Age Related Differences in Monocyte Subsets and Cytokine Pattern during Acute COVID-19-A Prospective Observational Longitudinal Study. *Cells.* 2021. **10**(12): 3373.

29 **Tan, S. Y., Cavanagh, L. L., d'Advigor, W., Shackel, N., Fazekas de St Groth, B. and Weninger, W.**, Phenotype and functions of conventional dendritic cells are not compromised in aged mice. *Immunol. Cell Biol.* 2012. **90**(7): 722–732.

30 **Metcalf, T. U., Wilkinson, P. A., Cameron, M. J., Ghneim, K., Chiang, C., Wertheimer, A. M., Hiscott, J. B. et al.**, Human Monocyte Subsets Are Transcriptionally and Functionally Altered in Aging in Response to Pattern Recognition Receptor Agonists. *J. Immunol.* 2017. **199**(4): 1405–1417.

31 **van Duin, D., Allore, H. G., Mohanty, S., Ginter, S., Newman, F. K., Belshe, R. B., Medzhitov, R. et al.**, Prevaccine determination of the expression of costimulatory B7 molecules in activated monocytes predicts influenza vaccine responses in young and older adults. *J. Infect. Dis.* 2007. **195**(11): 1590–1597.

32 **Chavez-Galan, L., Ruiz, A., Martinez-Espinosa, K., Aguilar-Duran, H., Torres, M., Falfan-Valencia, R., Pérez-Rubio, G. et al.**, Circulating Levels of PD-L1, TIM-3 and MMP-7 Are Promising Biomarkers to Differentiate COVID-19 Patients That Require Invasive Mechanical Ventilation. *Biomolecules.* 2022. **12**(3): 445.

33 **Schönrich, G. and Raftery, M. J.**, The PD-1/PD-L1 Axis and Virus Infections: A Delicate Balance. *Front. Cell Infect. Microbiol.* 2019. **9**: 207.

34 **Hou, J., Wang, S., Jia, M., Li, D., Liu, Y., Li, Z., Zhu, H. et al.**, A Systems Vaccinology Approach Reveals Temporal Transcriptomic Changes of Immune Responses to the Yellow Fever 17D Vaccine. *J. Immunol.* 2017. **199**(4): 1476–1489.

35 **Liu, C., Martins, A. J., Lau, W. W., Rachmaninoff, N., Chen, J., Imberti, L., Mostaghimi, D. et al.**, Time-resolved systems immunology reveals a late juncture linked to fatal COVID-19. *Cell.* 2021. **184**(7): 1836–1857. e22.

36 **Beshara, R., Sencio, V., Soulard, D., Barthélémy, A., Fontaine, J., Pinteau, T., Deruyter, L. et al.**, Alteration of Flt3-Ligand-dependent de novo generation of conventional dendritic cells during influenza infection contributes to respiratory bacterial superinfection. *PLoS Pathog.* 2018. **14**(10): e1007360.

37 **Pasquevich, K. A., Bieber, K., Günter, M., Grauer, M., Pötz, O., Schleicher, U., Biedermann, T. et al.**, Innate immune system favors emergency monopoiesis at the expense of DC-differentiation to control systemic bacterial infection in mice. *Eur. J. Immunol.* 2015. **45**(10): 2821–2833.

38 **Hao, Y., Hao, S., Andersen-Nissen, E., Mauck W. M., 3rd, Zheng, S., Butler, A., Lee, M. J. et al.**, Integrated analysis of multimodal single-cell data. *Cell.* 2021. **184**(13): 3573–3587. e29.

39 **Marongiu, L., Protti, G., Facchini, F. A., Valache, M., Mingozzi, F., Ranzani, V., Putignano, A. R. et al.**, Maturation signatures of conventional dendritic cell subtypes in COVID-19 suggest direct viral sensing. *Eur. J. Immunol.* 2022. **52**(1): 109–122.

40 **Huber, J. E., Ahlfeld, J., Scheck, M. K., Zaucha, M., Witter, K., Lehmann, L., Karimzadeh, H. et al.**, Dynamic changes in circulating T follicular helper cell composition predict neutralising antibody responses after yellow fever vaccination. *Clin. Transl. Immunology.* 2020. **9**(5): e1129.

41 **Pan, Y. G., Aiamkitsumrit, B., Bartolo, L., Wang, Y., Lavery, C., Marc, A., Holec, P. V. et al.**, Vaccination reshapes the virus-specific T cell repertoire in unexposed adults. *Immunity.* 2021. **54**(6): 1245–1256. e5.

42 **Puchinger, K., Castelletti, N., Rubio-Acero, R., Geldmacher, C., Eser, T. M., Deák, F., Paunovic, I. et al.**, The interplay of viral loads, clinical presentation, and serological responses in SARS-CoV-2 - Results from a prospective cohort of outpatient COVID-19 cases. *Virology.* 2022. **569**: 37–43.

Abbreviations: **CD**: cluster of differentiation · **COVID-19**: Coronavirus induced disease 2019 · **DC**: dendritic cell · **PBMC**: peripheral blood mononuclear cells · **PD-L1**: programmed death ligand 1 · **SARS-CoV-2**: Severe acute respiratory syndrome coronavirus 2 · **YF**: yellow fever

Full correspondence: Anne Krug, M.D., Institute for Immunology, Biomedical Center (BMC), LMU Munich, Großhaderner Str. 9, D-82152 Planegg-Martinsried, Germany
e-mail: anne.krug@med.uni-muenchen.de

Received: 15/7/2022
Revised: 18/10/2022
Accepted: 17/11/2022
Accepted article online: 20/11/2022